



HAL
open science

Alpha Decays Impact on Nuclear Glass Structure

S. Peugot, C. Mendoza, E.A. Maugeri, J.M. Delaye, R. Caraballo, T. Charpentier, M. Tribet, O. Bouty, C. Jegou

► **To cite this version:**

S. Peugot, C. Mendoza, E.A. Maugeri, J.M. Delaye, R. Caraballo, et al.. Alpha Decays Impact on Nuclear Glass Structure. *Procedia Materials Science* (Elsevier), 2014, 7, pp.252 - 261. 10.1016/j.mspro.2014.10.033 . cea-01729224

HAL Id: cea-01729224

<https://cea.hal.science/cea-01729224>

Submitted on 12 Mar 2018

HAL is a multi-disciplinary open access archive for the deposit and dissemination of scientific research documents, whether they are published or not. The documents may come from teaching and research institutions in France or abroad, or from public or private research centers.

L'archive ouverte pluridisciplinaire **HAL**, est destinée au dépôt et à la diffusion de documents scientifiques de niveau recherche, publiés ou non, émanant des établissements d'enseignement et de recherche français ou étrangers, des laboratoires publics ou privés.



Distributed under a Creative Commons Attribution - NonCommercial - NoDerivatives 4.0 International License



2nd International Summer School on Nuclear Glass Wasteform: Structure, Properties and Long-Term Behavior, SumGLASS 2013

Alpha decays impact on nuclear glass structure

S. Peugot^a, C. Mendoza^a, E.A. Maugeri^a, J.M. Delaye^a, R. Caraballo^a,
T. Charpentier^b, M. Tribet^a, O. Bouty^a, C. Jégou^a

^a CEA, DEN, Laboratoire d'Étude des Matériaux et Procédés Actif, 30207 Bagnols-sur-Cèze, France

^b CEA, IRAMIS, SIS2M, Laboratoire de Structure et Dynamique par Résonance Magnétique

Abstract

This paper reviews the main results on the long-term behavior of SON68 nuclear glass towards alpha decay accumulation. The effects of the radiation damage induced by alpha decay were investigated by doping a glass with a short-lived actinide ²⁴⁴Cm, by using ionic irradiations and by molecular dynamic simulations.

The analysis of the behavior of the glass structure subjected to ballistic effects with various spectroscopic studies has identified some local order changes around boron and silicon atoms. Moreover a modification of the medium-range order has also been demonstrated through changes in the bond angles between network formers and broadening of the ring size distributions, indicating increasing disorder of the glass structure. This structural evolution induced by alpha decays would be driven by the reconstruction of the glass disorganized by displacement cascades of the recoil nuclei, freezing a glass structure with a higher fictive temperature. This “ballistic disordering (BD) fast quenching” event induce a new glassy state characterized by a higher enthalpy state.

© 2014 The Authors. Published by Elsevier Ltd. This is an open access article under the CC BY-NC-ND license (<http://creativecommons.org/licenses/by-nc-nd/3.0/>).

Selection and peer-review under responsibility of the scientific committee of SumGLASS 2013

Keywords: radiation effects, alpha decay, glass structure, ballistic damage

* Corresponding author. Tel.: +33-466-796-529; fax: +33-466-797-708.
E-mail address: sylvain.peugot@cea.fr

1. Introduction

Borosilicate glass is the main material used to immobilize the high radioactive elements for dozen of hundreds of thousand years. To guarantee the long-term behavior of containment glasses in a nuclear waste repository, studies have been conducted since 1970 in Europe, in the USA and in Japan, on the effects of irradiation in nuclear glasses (Weber *et al.*, 1997).

The effect of alpha decays on the macroscopic properties of the French borosilicate glass (SON68) glass was largely studied and recently reviewed in (Peugeot *et al.*, 2014). It was shown that the accumulation of alpha decay diminishes the hardness (by about 30%) and Young's modulus (by 15 to 30%) and increases the fracture toughness (by 50 to 80%) (Inagaki *et al.*, 1992, Matzke & Vernaz, 1993, Matzke, 1997, Peugeot, Cachia, *et al.*, 2006). A small glass swelling of around 0.5-0.6% was also observed. External irradiation studies and molecular dynamics simulation of the accumulation of displacement cascades have also shown swelling and modification of the mechanical properties of simple glasses with the deposited energy dose, followed by stabilization (Bureau *et al.*, 2008, Delaye *et al.*, 2011, Peugeot *et al.*, 2014). The comparison of the macroscopic evolutions of the Cm doped glass with those obtained for glasses irradiated with light or heavy ions suggests that the macroscopic evolutions are induced by the nuclear interactions induced by the recoil nuclei of alpha decay.

In order to understand the atomistic origin of the macroscopic properties variation of SON68 glasses under accumulation of alpha decays some structural studies were started more recently (de Bonfils *et al.*, 2007, de Bonfils *et al.*, 2010, Bureau *et al.*, 2008, Delaye *et al.*, 2011, Mendoza *et al.*, 2012, Peugeot *et al.*, 2013). The objective of this paper is to review the structural evolution observed and discuss the associated damage mechanism.

2. Materials and methods

A multifaceted approach was adopted (Peugeot *et al.*, 2014) for evaluating the effects of alpha decays on the glass properties and structure, consisting mainly of specific laboratory-scale experiments simulating the aging of containment glasses, and atomistic simulations designed to understand the observed phenomena at atomic scale.

2.1. ^{244}Cm -doped glasses

Doping a glass with short-lived actinides is the most representative methods used to simulate the effects of alpha decays because the entire glass volume is irradiated in the same way as in a nuclear glass, involving all the components of alpha disintegration: recoil nuclei and alpha particles. Between 2001 and 2007, four batches of SON68 glass (R7T7-type glass in which fission products are simulated by nonradioactive elements) doped to 0.04, 0.4, 1.2 and 3.25 wt% $^{244}\text{CmO}_2$ and one batch of ISG glass doped to 0.7% wt% $^{244}\text{CmO}_2$ were fabricated in the Atalante high-level waste laboratory (Peugeot, Cachia, *et al.*, 2006, Mendoza *et al.*, 2012). They will be called XCmSON68 or 0.7CmISG in the paper where X is the weight percent of $^{244}\text{CmO}_2$ in the glass. Their macroscopic properties (density, modulus of elasticity, hardness, fracture toughness, initial alteration rate), and their microstructure and structure were examined periodically over time. Their chemical compositions and the elaboration process are described in detail in reference (Peugeot *et al.*, 2014). Their periodical characterizations allowed investigating the effects of alpha decay doses corresponding to 100000 years of disposal of nuclear glasses.

2.2. External irradiation

The second area of study uses nonradioactive (“inactive”) surrogate glass compositions in which irradiation stresses were simulated by external irradiation with ions. Different types of irradiation can simulate the different components of alpha disintegration (recoil nucleus and alpha particle) and thus dissociate electronic effects from nuclear effects. Different types of external irradiation by He, Kr and Au ions (Peugeot, Noel, *et al.*, 2006) were implemented at IPN Orsay and IPN Lyon. This paper will illustrate the glass structural evolutions from gold ions irradiation results whose irradiation parameters are summarized in table 1.

In addition to SON68 glass, simplified glasses were also irradiated to facilitate structural analyses (Bureau *et al.*, 2008, de Bonfils *et al.*, 2007, de Bonfils *et al.*, 2010). It was first necessary to check that irradiation led to similar

changes in the glass properties (de Bonfils *et al.*, 2010). Table 2 summarizes the main simplified glass compositions investigated.

Table 1. Ion irradiation conditions, Enucl and Eelec correspond to the mean energy deposited by nuclear and electronic interaction in the irradiated zones

Irradiation by Au ions (multi-energy mode)							
Fluence at/cm ²	(Energy)	1.9E+11 (1)	6.1E+11 (1)	1.1E+12 (1)	2.4E+12 (1)	6.1E+12 (1)	4.6E+13 (1)
	(MeV)	5.8E+11 (3.5)	1.8E+12 (3.5)	3.3E+12 (3.5)	7.3E+12 (3.5)	1.8E+13 (3.5)	1.4E+14 (3.5)
		1.4E+12 (7)	4.2E+12 (7)	7.6E+12 (7)	1.7E+13 (7)	4.2E+13 (7)	3.2E+14 (7)
<i>E</i> _{nucl}	(keV/cm ³)	1.6E+19	5.0E+19	9.0E+19	2.0E+20	5.0E+20	3.8E+21
<i>E</i> _{elec}	(keV/cm ³)	5.5E+19	1.7E+20	3.1E+20	6.8E+20	1.7E+21	1.3E+22

Table 2. Chemical composition of the main glass studied

mol%	SiO ₂	Na ₂ O	B ₂ O ₃	Al ₂ O ₃	CaO	ZrO ₂	Others
CJ1	67.7	14.2	18.1				
ISG or CJ4	60.1	12.6	16.0	3.8	5.7	1.7	
SON68	52.8	11.3	14.1	3.4	4.6	1.5	12.3

2.3. Atomistic modeling

Molecular dynamics (MD) simulations was used to investigate the ballistic damage induced by the recoil nuclei (RN) emitted by alpha disintegrations. Heavy nuclei were accelerated to energies ranging from a few electron-volts to 70 keV in the sodium borosilicate glass CJ1 (table 2). Simulating displacement cascades arising from projectiles of different energies shorten the computation time while ensuring the representativeness of the phenomena observed over the entire energy range (Delaye & Ghaleb, 2005a, b). Accumulating multiple series of displacement cascades made it possible to simulate ballistic doses corresponding to about 100000 years of glass storage (Bureau *et al.*, 2008, Delaye *et al.*, 2011).

3. Evolution the glass structure

The effect of irradiation on the structure of the borosilicate glasses was investigated by combining different techniques (DSC, Raman, NMR and XANES spectroscopies) describing the structural organization of the glass at macroscopic scale and at atomic scale by characterizing the local and medium-range order.

The Raman spectra of SON68 Cm doped glasses show few evolutions with the accumulation of alpha decay dose (figure 1). The spectra confirm that no secondary phases (neither crystalline nor amorphous) are formed under such irradiation conditions. Another important point to notice is that the spectra of the Cm SON68 doped glasses damaged more than by $2 \times 10^{18} \alpha \cdot g^{-1}$ are exactly the same, which is consistent with the stabilization of macroscopic properties discussed previously. The slight spectral differences between the undamaged ($1.8 \times 10^{17} \alpha \cdot g^{-1}$) and damaged glasses concern the bands situated at around 500 cm^{-1} (Si-O-Si mixed bending and rocking vibration) and $900\text{-}1200 \text{ cm}^{-1}$ (Si-O stretching vibration in SiO₄ tetrahedra). A shift to higher wavenumber of around 10 cm^{-1} of the band situated around 500 cm^{-1} is observed with dose which suggests a decrease of the mean Si-O-Si bond angle (Peugeot *et al.*, 2014). It corresponds to a decrease of the mean Si-O-Si angle of around 2° according to the relation of 5.5 cm^{-1} per degree obtained by Okuno *et al.* (Okuno *et al.*, 1999). Moreover the shape of the Qn band changed slightly with irradiation with suggests a modification of the connectivity of silica tetrahedra.

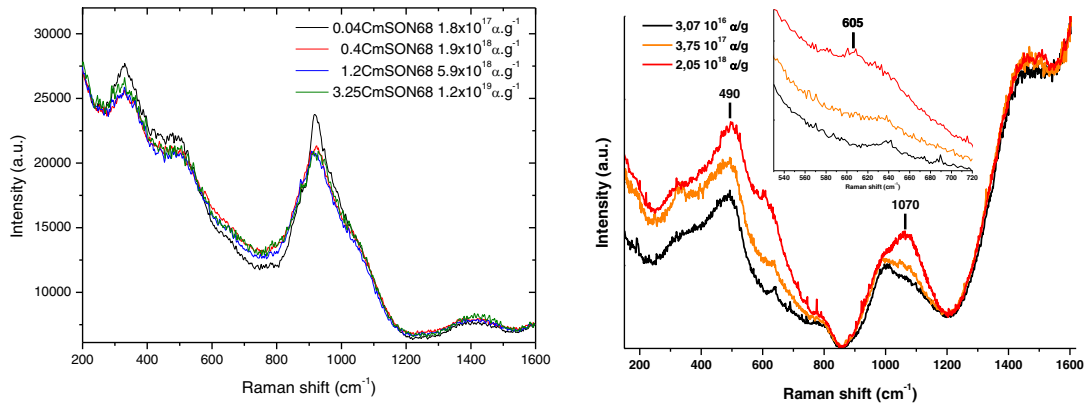


Fig. 1. (left) Raman spectra of the CmSON68 glass, (right) Raman spectra of the 0.7CmISG glass

For 0.7CmISG glass a strong signal of Cm³⁺ luminescence interferes with the Raman spectra above 1200 cm⁻¹, preventing the interpretation of that part of the spectra (figure 1). Three main modifications of the Raman spectrum can be observed. There is first a shift of the band at 490 cm⁻¹ towards the higher wavenumbers which also suggests a decrease of the Si-O-Si mean angle. Secondly an increase of the intensity of a band at 605 cm⁻¹ is observed that could reflect the emergence of the D2 band that corresponds to the Si-O-Si bonds vibration in three members silica rings (Sharma *et al.*, 1981). Finally, there is a strong increase with the alpha decay dose of the 1070 cm⁻¹ band intensity. This band is usually attributed in borosilicate (Parkinson *et al.*, 2008, Windisch *et al.*, 2011, Peuket *et al.*, 2013) glasses to the stretching vibration of the Si-O bonds in SiO₄ tetrahedra with three bridging oxygen atoms (Q3 band). It traduced a modification of the connectivity of silica tetrahedra.

Raman spectroscopy was also applied on externally irradiated glasses. Similar evolutions of the Raman bands were observed for CJ1 and ISG glass irradiated by gold ions (de Bonfils *et al.*, 2010, Mendoza *et al.*, 2012). Indeed a shift of around 10 cm⁻¹ of the band situated around 500 cm⁻¹ was observed (figure 2) suggesting a decrease of the mean angle between the silicon tetrahedra. Moreover, this band shift stabilizes for a deposited nuclear energy dose of around 10²¹ keV.cm⁻³ which correspond to around 5x10¹⁸ alpha.g⁻¹. Concerning the Qn Raman band it is also interesting to notice that on CJ1 samples irradiated with gold ions this band seems to evolve with the dose in the direction of a slightly less polymerized glass (de Bonfils *et al.*, 2010).

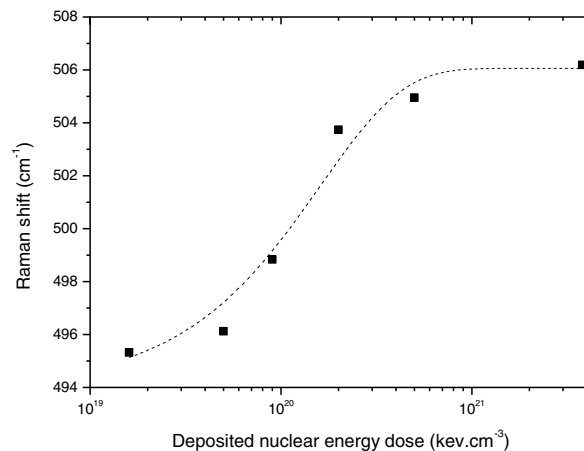


Fig. 2. Si-O-Si bending band position versus deposited nuclear energy dose for CJ1 glass irradiated by gold ions. The dash curve was obtained by fitting the experimental data with an exponential law.

NMR spectroscopy was also applied on Au ions (highest fluence of table 1) irradiated ISG glass powder of fine particle size ($<2 \mu\text{m}$) to evaluate the modifications of the local order around the main glass nuclei, ^{29}Si , ^{23}Na , ^{27}Al , ^{11}B (Peuguet *et al.*, 2014). BO_4 are partially converted into BO_3 with Au irradiation, with a decrease of BO_4 species from 50 to 35% (figure 3). The ^{29}Si spectra in figure 3 are characteristic of Q_3 and Q_4 units (SiO_4 tetrahedra with respectively 3 and 4 bridging oxygen atoms). A slight shift of the irradiated glass spectrum was observed toward smaller chemical shifts, which corresponds to a slightly higher proportion of Q_3 species and thus to a lower polymerization of silicate units. Moreover a slight shift of the Na spectra was observed with irradiation which traduces a decrease in the Na-O distance and so a modification of the role of sodium atoms in the glassy structure. We can also notice that a reduction in the boron coordination number under gold ions irradiation was observed by XANES spectroscopy in CJ1, ISG and to a lower extent in SON68 glass (Bureau, 2008).

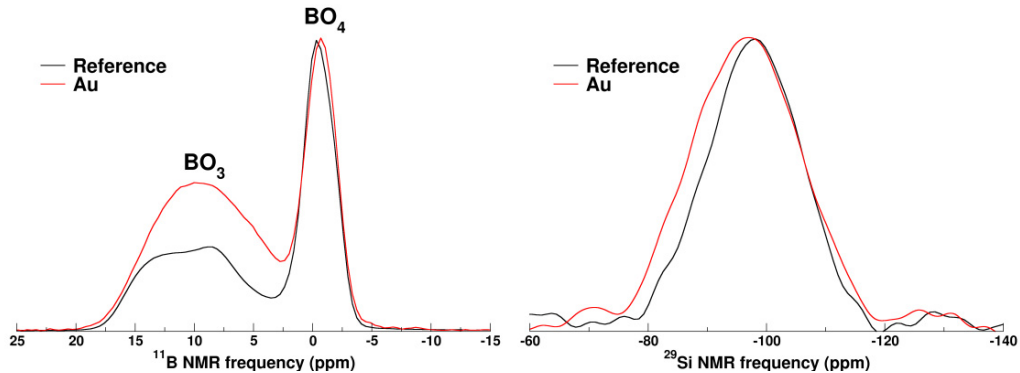


Fig. 3. ^{11}B (left) and ^{29}Si (right) MAS spectra of CJ4 glass before (reference) and after irradiation by gold ions (Au)

Atomistic modeling studies of accumulation of displacement cascades in CJ1 glass showed a strong regenerative capacity of the glass network after structural disorganization by the recoil nuclei (Bureau, 2008). Nevertheless, a few short-range order structural modifications were observed, notably the conversion of BO_4 into BO_3 units and an increase in the concentration of non-bridging oxygen atoms (figure 4). In addition to the modifications in the local order around the cations, molecular dynamics studies (Delaye *et al.*, 2011) also revealed an evolution of the medium-range order. A modification in the bond angles between network formers was observed; in particular a decrease of the mean Si-O-Si bond angle of around 6° , so a behaviour similar to the one observed on Cm doped and externally irradiated glasses. Moreover a broadening of the ring-size distributions was noticed in which an increase of the number of three member's rings can be observed. With the accumulation of nuclear interactions, the structural evolutions observed by MD (local order and medium range order) stabilize when the deposited nuclear energy dose is around $10^{21} \text{keV}\cdot\text{cm}^{-3}$ (Delaye *et al.*, 2011). It is thus interesting to notice that these structural evolutions observed with MD simulations are in very good agreement with the experimental findings described previously which confirms that the structural evolutions observed are mainly induced by the ballistic effects.

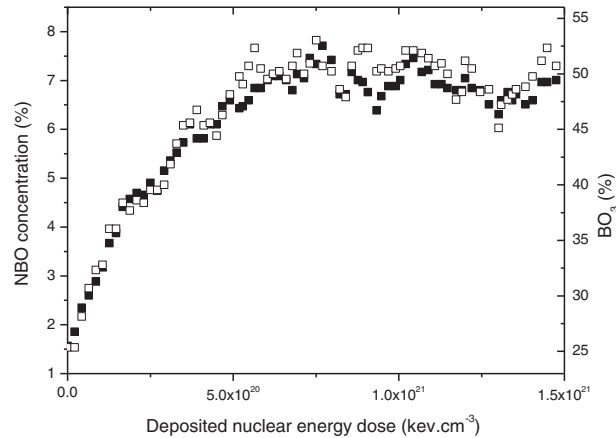


Fig. 4. Evolution of the percentage of nonbridging oxygen atoms (full square) and tricoordinate boron atoms (open square) in CJ1 glass subjected to a series of 600 eV cascades

Moreover DSC analyses were recently performed on Cm-doped glass specimens to evaluate the fictive temperature (T_f) of Cm doped SON68 glass and its evolution versus the alpha decay dose (Maugeri *et al.*, 2012) (figure 5). This figure shows an increase in T_f of CmSON68 glass with alpha self-irradiation, which means that the accumulation of alpha disintegrations results in freezing a vitreous state with a higher enthalpy state than during the initial glass thermal cycle. A high fictive temperature usually indicates that the glass was fast quenched. This result suggests that the irradiated state could be similar to a very high quenching rate glassy state. We can notice that all the structural evolutions under irradiation previously described are consistent with the ones usually observed with increasing the glass temperature or the thermal quenching rate (Peugeot *et al.*, 2013). This figure also shows that above an alpha decay dose of about $4 \times 10^{18} \alpha \cdot g^{-1}$, the fictive temperature remains constant, confirming the formation of a new structure that remains stable with respect to further accumulation of alpha decay. The variation in the fictive temperature of the glass versus the alpha decay dose is in full agreement with the density variation, which corroborate the idea that changes in the glass macroscopic properties are related to a structural reorganization.

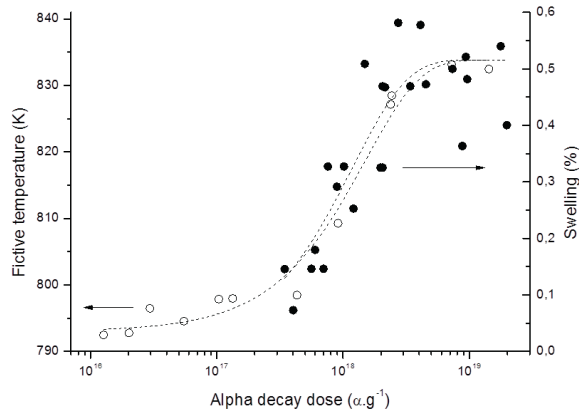


Fig. 5. Fictive temperature (open circle) and swelling (full circle) versus the alpha decay dose in CmSON68 glass. The dash curves were obtained by fitting the experimental data with an exponential law.

4. Origin of the evolution of the glass structure

The preceding paragraphs described changes in the structure of borosilicate glasses when subjected to various irradiation conditions. The agreement observed on the evolution of macroscopic properties and structural parameters when considering the nuclear damage induced by alpha decays, ion irradiations and MD studies suggest that nuclear or ballistic interactions are responsible of these modifications. The driver of this structural evolution could be the reconstruction of the glass, disorganized by displacement cascades, different from the initial construction of the material by quenching of the melt and annealing of the glass. As indicated by MD simulations, the displacement cascade generated by a recoil nucleus creates significant structural disorder during the ballistic phase, here called ballistic disordering (BD). Because the cascade is isolated within a material at room temperature, the glass cannot relax to its initial state and its structure is relaxed only by the thermal energy dissipated by the displacement cascade, which correspond to the quenching of the ballistic disordering state. The glass structure after a recoil nuclei event is then similar to a structure frozen from a very high temperature state, because it cannot reach a greater relaxed vitreous state.

This reasoning corresponds to the idea that irradiation increases the fictive temperature of the glass, as previously suggested by Simon (Simon, 1957), Geissgerber (Geissberger & Galeener, 1983), and Devine (Devine, 1994) to account for radiation-induced changes in amorphous silica. In this hypothesis, some of the BO_4 units destabilized by the displacement cascade more readily form BO_3 units; this is consistent with the shift in the BO_4/BO_3 equilibrium toward a higher percentage of BO_3 units observed at high temperatures in sodium borosilicate glass (Stebbins & Ellsworth, 1996, Sen, 1999, Wu & Stebbins, 2010, Angeli *et al.*, 2012). In addition, the hypothesis of local thermal quenching of the BD is consistent with a slight depolymerization of the silicate network.

The DSC analysis of the Cm-doped SON68 glass corroborated this idea by demonstrating an increase in the fictive temperature of the glass with the alpha decay dose (figure 5). This study also shows that above an alpha decay dose of about $4 \times 10^{18} \alpha \cdot \text{g}^{-1}$ the fictive temperature of the glass remains constant, confirming the formation of a new structure that remains stable with respect to further accumulation of alpha decay.

Several studies have recently been initiated to refine the underlying analogy between the structural state created by a displacement cascade and major thermal quenching (Bureau, 2008, Bibent *et al.*, 2009, Peuket *et al.*, 2013). The thermal history of the glass at the core of a displacement cascade was determined by molecular dynamics calculations (Bureau, 2008). The ballistic phase is characterized by agitation that was quantified by a pseudo-temperature calculated from the kinetic energy of the atoms. This is relative to local motion, but the term “local temperature” is abusive in that the structure passes through a transient state far from equilibrium. In the interval between 0.5 and 5 picoseconds after the initiation of the displacement cascade during which most of the glass structure forms again (Delaye & Ghaleb, 2000) the quenching rates in the cells inside the displacement cascade are often higher than $10^{14} \text{K} \cdot \text{s}^{-1}$, and thus exceed the quenching rate at which the initial glass was prepared.

It is therefore reasonable to assume that at the core of a displacement cascade a “thermal effect” occurs on the glass structure, in the sense that the zone damaged by high-energy atoms (ballistic disordering, BD) is then quenched at a higher rate than the initial glass quenching rate. The final equilibrium structure corresponds to a glass structure prepared at a higher quenching rate, and will thus have a higher fictive temperature. Given the very short time scales involved, however, it is unlikely that the glass can reach an equilibrium state at high-temperature during the relaxation phase following the BD. It is more likely that the structural state arising from the displacement cascade is not due exclusively to the effect of thermal quenching on a material stabilized at high temperature, but probably also reflects a poorly relaxed ballistic disorder. Recently two studies, one experimental (Peuket *et al.*, 2013), one by MD simulations (Delaye *et al.*, 2014) confirmed that ballistic processes induce specific structural effects that are not reproduced by accelerated quenching rates. Indeed the Raman spectra of figure 6 show that some medium range order modifications, i.e. a shift of the bending band of Si-O-Si bond and the appearance of D2 band, are only observed after gold irradiation and not after the increase of the quenching rate. This could suggest that the irradiated state is not obtained from an equilibrated melt but also that the frozen surrounding of the ballistic tracks constrains the reconstruction of the damaged glass structure by the modifying the glass medium range order.

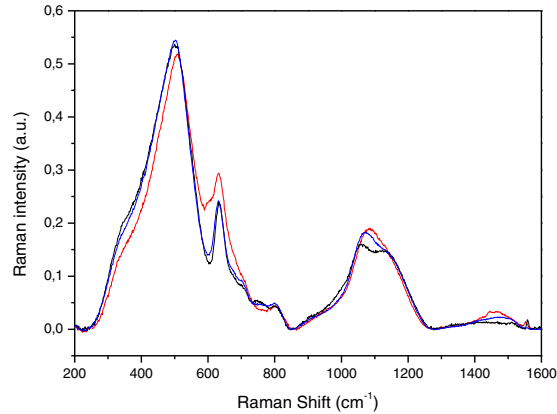


Fig. 6. Raman spectra of CJ1 glasses with quenching rate of 0.1 (black) and 3×10^4 (blue) $\text{K} \cdot \text{min}^{-1}$ and after gold ions irradiation (red)

We have attempted to describe the structural changes in the glass under ballistic irradiation by means of a model of accumulation of local quenching of the zones disorganized by the passage of recoil nuclei, called model of ballistic disordering fast quenching accumulation (Maugeri *et al.*, 2012). In this phenomenological representation, the passage of a recoil nucleus in a region of the glass would result in the formation of a new structure defined by the thermal history following the displacement cascade. The accumulation of such events throughout the glass volume would gradually lead to the formation of a new glass with a higher fictive temperature. The passage of another recoil nucleus in a zone already affected by an earlier projectile would temporarily disorganize the glass structure during the cascade, but the structure would form again in the same way as after the first passage because the factors controlling the formation of the final structure are equivalent, i.e. the displacement cascade morphology and its thermal history.

With these hypotheses the evolution of a structural or macroscopic property of a glass specimen subjected to alpha self-irradiation can be described by computing the variation, as a function of the alpha decay dose, of the volume fraction damaged once. This corresponds to a direct impact damage model which predicts variations according to an exponential law (equation 1) that is consistent with the experimental observations reported above. A recent study by Griscom and Weber (Griscom & Weber, 2011) in which plutonium-doped glass was characterized by electron paramagnetic resonance also concluded that the glass structural damage varied as an exponential function of the dose.

$$\frac{\Delta T_f}{T_{f_0}} = T_{f_{Sat}} (1 - \exp(-V_c D)) \quad (1)$$

where T_{f_0} is the initial fictive temperature of the glass, $T_{f_{Sat}}$ its fictive temperature after saturation, V_c the unit volume damaged individually by each recoil nucleus, and D the alpha decay dose.

In addition, the fit of the density and fictive temperature variations with the alpha decay dose give V_c values of 280 and 240 nm^3 , respectively, near the value of 270 nm^3 determined by molecular dynamics simulation from analysis of the displacement cascade morphology (Peugot, Cachia, *et al.*, 2006, Maugeri *et al.*, 2012). The experimental variations of the properties are thus compatible with the proposed phenomenological model of accumulations of ballistic disordering fast quenching events created by alpha decay recoil nuclei.

5. Conclusion

By using a multifaceted approach based on Cm doped glasses, ionic irradiations and MD simulations, the effect of alpha decays on nuclear glass structure was evaluated. Some changes in the local order around the main glass elements together with modifications of the medium range order were observed. The local order changes are similar to the ones usually observed with increasing the glass temperature or quenching rate, which suggest that ballistic effects could be very similar to a thermal effect. But the medium range order modifications suggest that ballistic processes induce specific structural modifications that do not seem to be reproduced by accelerated quenching rate. A “ballistic disordering (BD) fast quenching” model is proposed to account for the glass structural evolution under alpha decays.

Acknowledgements

This project was carried out under a research program jointly funded by CEA and AREVA.

References

- Angeli, F., Villain, O., Schuller, S., Charpentier, T., de Ligny, D., Bressel, L. & Wondraczek, L. (2012). *Physical Review B: Condens. Matter Mater. Phys.* **85**.
- Bibent, N., Faivre, A., Ferru, G., Bantignies, J. L. & Peugeot, S. (2009). *J. Appl. Phys.* **106**, 063512.
- Bureau, G. (2008). thesis, Université Pierre et Marie Curie, Paris.
- Bureau, G., Delaye, J. M., Peugeot, S. & Calas, G. (2008). *Nuclear Instruments & Methods in Physics Research Section B-Beam Interactions with Materials and Atoms* **266**, 2707-2710.
- de Bonfils, J., Panczer, G., de Ligny, D., Peugeot, S. & Champagnon, B. (2007). *Journal of Nuclear Materials* **362**, 480-484.
- de Bonfils, J., Peugeot, S., Panczer, G., de Ligny, D., Henry, S., Noel, P. Y., Chenet, A. & Champagnon, B. (2010). *Journal of Non-Crystalline Solids* **356**, 388-393.
- Delaye, J. M. & Ghaleb, D. (2000). *Physical Review B* **61**, 14481-14494.
- Delaye, J. M. & Ghaleb, D. (2005a). *Physical Review B* **71**, 224203.
- Delaye, J. M. & Ghaleb, D. (2005b). *Physical Review B* **71**, 224204.
- Delaye, J. M., Peugeot, S., Bureau, G. & Calas, G. (2011). *Journal of Non-Crystalline Solids* **357**, 2763-2768.
- Delaye, J. M., Peugeot, S., Calas, G. & Galoisy, L. (2014). *Nuclear Instruments & Methods in Physics Research Section B-Beam Interactions with Materials and Atoms* **326**, 256-259.
- Devine, R. A. B. (1994). *Nuclear Instruments & Methods in Physics Research Section B-Beam Interactions with Materials and Atoms* **91**, 378-390.
- Geissberger, A. E. & Galeener, F. L. (1983). *Phys. Rev. B: Condens. Matter Mater. Phys.* **28**, 3266-3271.
- Griscom, D. L. & Weber, W. J. (2011). *Journal of Non-Crystalline Solids* **357**, 1437-1451.
- Inagaki, Y., Furuya, H., Ono, Y., Idemitsu, K., Banba, T., Matsumoto, S. & Muraka, S. (1992). *Scientific Basis for Nuclear Waste Management XVI Symposium*, 191-198.
- Matzke, H. (1997). *Université d'été du CEA-Valrhô*. Mejanne Le Clap: Odyssee.
- Matzke, H. & Vernaz, E. (1993). *Journal of Nuclear Materials* **201**, 295-309.
- Maugeri, E. A., Peugeot, S., Staicu, D., Zappia, A., Jegou, C. & Wiss, T. (2012). *Journal of the American Ceramic Society* **95**, 2869-2875.
- Mendoza, C., Peugeot, S., Bouty, O., Caraballo, R. & Jégou, C. (2012). *Procedia Chemistry* **7**, 581-586.
- Okuno, M., Reynard, B., Shimada, Y., Syono, Y. & Willaime, C. (1999). *Physics and Chemistry of Minerals* **26**, 304-311.
- Parkinson, B. G., Holland, D., Smith, M. E., Larson, C., Doerr, J., Affatigato, M., Feller, S. A., Howes, A. P. & Scales, C. R. (2008). *Journal of Non-Crystalline Solids* **354**, 1936-1942.
- Peugeot, S., Cachia, J. N., Jegou, C., Deschanel, X., Roudil, D., Broudic, V., Delaye, J. M. & Bart, J. M. (2006). *Journal of Nuclear Materials* **354**, 1-13.
- Peugeot, S., Delaye, J. M. & Jégou, C. (2014). *Journal of Nuclear Materials* **444**, 76-91.

- Peuget, S., Maugeri, E. A., Charpentier, T., Mendoza, C., Moskura, M., Fares, T., Bouty, O. & Jégou, C. (2013). *Journal of Non-Crystalline Solids* **378**, 201-212.
- Peuget, S., Noel, P. Y., Loubet, J. L., Pavan, S., Nivet, P. & Chenet, A. (2006). *Nuclear Instruments & Methods in Physics Research Section B-Beam Interactions with Materials and Atoms* **246**, 379-386.
- Sen, S. (1999). *Journal of Non-Crystalline Solids* **253**, 84-94.
- Sharma, S. K., Mammone, J. F. & Nicol, M. F. (1981). *Nature* **292**, 140-141.
- Simon, I. (1957). *J. Am. Ceram. Soc.* **40**, 150-153.
- Stebbins, J. F. & Ellsworth, S. E. (1996). *Journal of the American Ceramic Society* **79**, 2247-2256.
- Weber, W. J., Ewing, R. C., Angell, C. A., Arnold, G. W., Cormack, A. N., Delaye, J. M., Gscom, D. L., Hobbs, L. W., Navrotsky, A., Price, D. L., Stoneham, A. M. & Weinberg, M. C. (1997). *Journal of Material Society* **12**, 1946-1978.
- Windisch, C. F., Jr., Pierce, E. M., Burton, S. D. & Bovaird, C. C. (2011). *Journal of Non-Crystalline Solids* **357**, 2170-2177.
- Wu, J. & Stebbins, J. F. (2010). *Journal of Non-Crystalline Solids* **356**, 2097-2108.